Chapter 2 Basic Theory

2.1 Optical Bottle Beam

From introduction of the thesis in Chapter 1, many different ways of generating optical bottle beam had been reported. Here we use the method that is assembly of an axicon and a positive lens. One of these optical elements, axicon, whose geometric shape is shown in Figure 2.1.

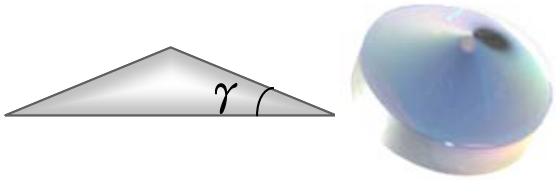

Fig. 2.1 Geometric shape of an axicon.

An axicon, introduced by McLeod in 1954 [32], is a refractive or diffractive optical element for imaging axially symmetric light to a continuous range of points extended along axis. There are many different kinds of axicons but probably the most important one is a glass cone, with an angle γ between the conical surface and flat surface. It has the property that a point source on its axis of revolution is imaged to a range of points along its axis. Therefore, the name axicon means axis image. Recently, the axicon has attracted to be an optical element to generate a non-diffracting light, commonly known as non-diffracting Bessel beam [33] [34]. A Bessel beam is formed after a beam impinges upon an axicon. The beam is propagating-invariant in a particular region characterized by Z_{max}, which depends on the angle of the cone, means parameter γ. Its geometric ray trace is shown in Figure 2.2. And from geometric optics, we can estimate ray open angle $\theta = (n-1)\,\gamma$ and Z_{max} is about w_0/θ, where n is the refractive index of the axicon material, γ is the angle of the axicon's cone, and w_0 is the spot size of incident beam.

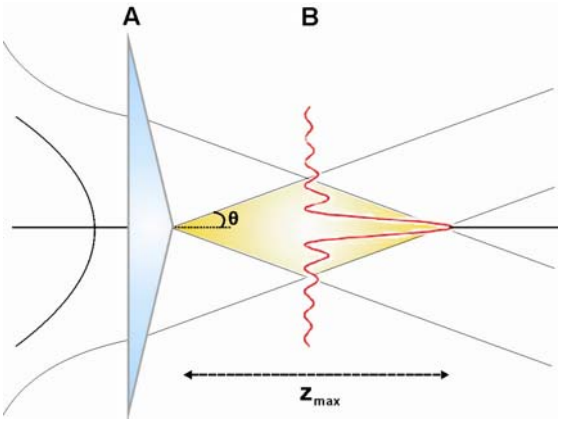

Fig. 2.2 Ray trace of axicon

When a beam passes through the axicon, the phase of output light field will be changed. Latter we would estimate what its function of phase changed to understand what the axicon influences the light field. The phase shift depends on which trace of light through the axicon element, and the diagram is shown in Figure 2.3.

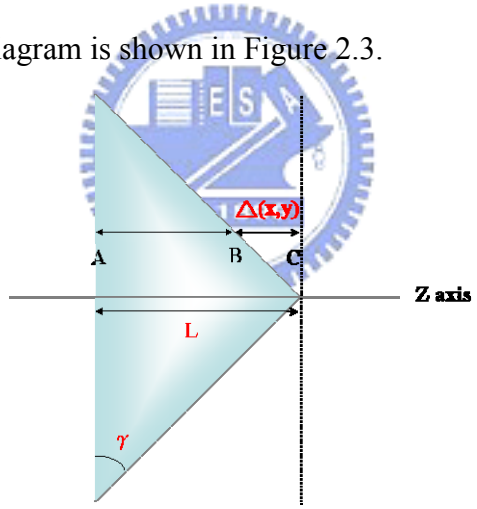

Fig. 2.3 Phase change on passing through the axicon.

When passed through the axicon, the light field would gain a transmittance coefficient $\tau(x,y)$, represented as $Exp(i\Phi(x,y))$, where $\Phi(x,y)$ is the phase function of positions. Then phase function after the axicon can be expressed as:

$$\Phi(x,y) = k\,\Delta(x,y) + k\,n(L - \Delta(x,y)), \tag{2.1.1}$$

where k is wave number, $\Delta(x,y)$ is distance between positions B and C, L is thickness of axicon, and n is the refractive index of axicon material. The phase function represents the

phase change of the optical path from point A to point C. Point A to point B is inside the axicon material portion, and B to C is in the air portion. From the geometric cone shape of axicon, we can estimate the distance in the air portion as:

$$\Delta(x,y) = \sqrt{x^2 + y^2}\ \tan\gamma = r\tan\gamma\ , \tag{2.1.2}$$

where γ is the angle of cone, and r is the cross sectional distance from the axis of axicon. And the phase function can be shown as

$$\Phi(x,y) = \Phi(r) = -k\,(n-1)\,r\tan\gamma + knL\ . \tag{2.1.3}$$

We assume L, the thickness of the axicon, is too small to be neglected, and the transmittance coefficient after passing through the axicon is

$$\tau(r) = exp\left(-i\,k\,(n-1)\,r\tan\gamma\right). \tag{2.1.4}$$

For the same reason, when light passed through a lens, the transmittance coefficient $\tau'(r)$ can be expressed as [35]

$$\tau'(r) = exp\left(-ik\frac{r^2}{2f}\right), \tag{2.1.5}$$

where f is the focal length of the lens. By putting a focus lens behind the axicon at a distance $f < Z = Z_0 < Z_{max}$, the collimated Gaussian beam will reconstruct to form the optical bottle beam in the range of Z_1 and Z_2, shown in Figure 2.4 [17].

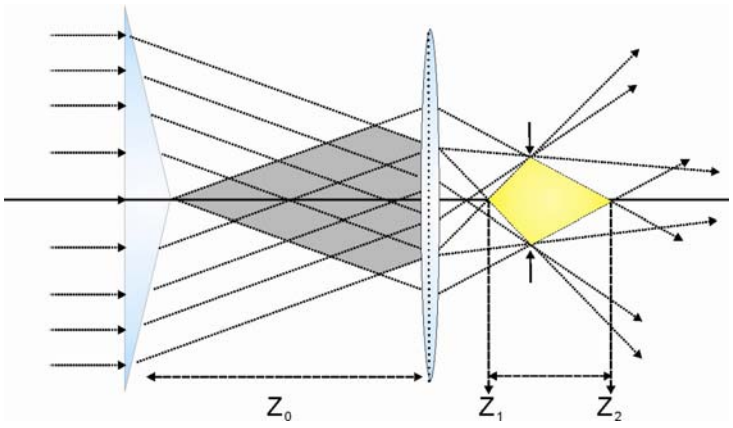

Fig. 2.4 Ray trace of optical bottle beam by using assembly of an axicon with a focus lens.

2.1.1 Fresnel-Kirchhoff's Diffraction Formula

We considered the propagation of a general beam of light with a finite transverse dimension, and described the beam propagation by decomposing the light beam into a superposition of plane waves. Based on the principle of superposition, all waves of finite extent can be expressed in terms of a linear combination of plane waves, so the beam propagation behavior can be described the superposition of these wave components. This approximation is known as *Fresnel-Kirchhoff's diffraction integral*, and below is its proof.

At first, we considered the propagation of a general beam of light along *z*-axis, and the diagram is shown in Figure 2.5.

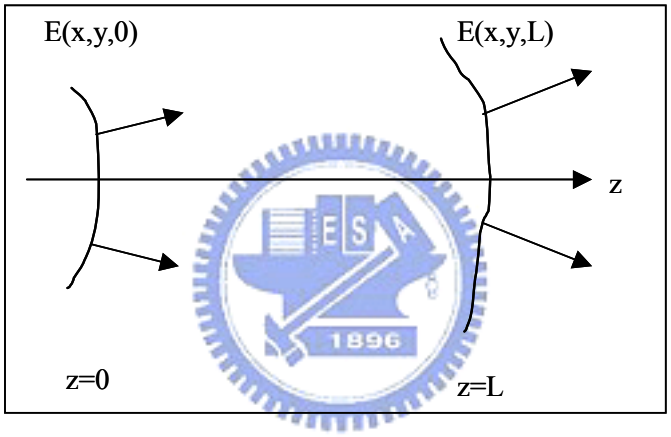

Fig. 2.5 The propagation of beam along z-axis from z = 0 to z = L.

At $z = 0$, we can write the amplitude as a Fourier integral of plane wave in following:

$$E(x,y) = \iint A(k_x,k_y)\exp(ik_x x + ik_y y)dk_x dk_y , \tag{2.1.6}$$

where $A(k_x,k_y)$ is the amplitude of the (k_x, k_y) plane wave component. After propagating a distance z, the field amplitude of beam can be written as

$$E(x,y,z) = \iint A(k_x,k_y)\exp(ik_x x + ik_y y)\exp(ik_z z)dk_x dk_y , \tag{2.1.7}$$

where k_z is the wave vector along the z direction. Its components must satisfy

$$k_x^2 + k_y^2 + k_z^2 = \left(\frac{\omega}{c}n\right)^2 \equiv k^2 , \tag{2.1.8}$$

where ω is the angular frequency, n is the index of refraction, k is the wave number of the light in the medium, and c is the speed of light. Under the paraxial approximation, we considered k_x, $k_y << k$, and k_z can be expressed as

$$k_z = k - \frac{k_x^2 + k_y^2}{2k}. \tag{2.1.9}$$

And Equation (2.1.7) can be simplified as:

$$E(x,y,z) = \iint A(k_x, k_y) exp(ikz - i\frac{k_x^2 + k_y^2}{2k^2} z) exp(ik_x x + ik_y y) dk_x dk_y, \tag{2.1.10}$$

where $A(k_x,k_y)$ is the amplitude of wave vector k, so Equation (2.5) becomes

$$E(x,y,z) = \frac{1}{(2\pi)^2} \iint dx'dy' \iint E(x',y') e^{ik_x(x-x')+ik_y(y-y')} e^{ikz - i\frac{k_x^2+k_y^2}{2k} z} dk_x dk_y. \tag{2.1.11}$$

After a trivial mathematical manipulation, Eq. (2.1.11) can be reduced to

$$E(x,y,z) = -\frac{i}{\lambda z} e^{ikz} \iint E(x',y') e^{ik\frac{(x-x')^2+(y-y')^2}{2z}} dx'dy'. \tag{2.1.12}$$

This is known as the *Fresnel-Kirchhoff diffraction integral.* And latter the *Fresnel Kirchhoff diffraction integral* can be reproduced with a slight change of notation.

We then consider the propagation of input beam passing through a general optical system that includes lens-like elements, and the diagram is shown in Figure. 2.6

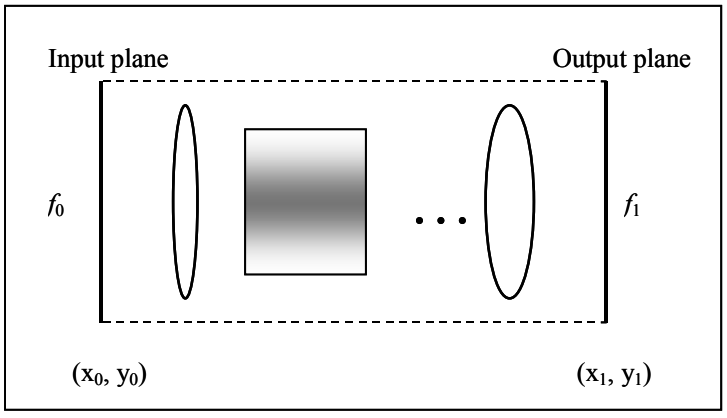

Fig. 2.6 A cascade of lenslike (paraxial) elements with an overall *ABCD* matrix.

We assumed the input field $f_0(x,y)$ and the output field $f_1(x,y)$ at $z=L$ through optical system can be expressed in terms of *ABCD* matrix. The *Fresnel Kirchhoff diffraction integral*

becomes:

$$f_1(x_1, y_1, L) = -\frac{ik}{2\pi L}\iint f_0(x_0, y_0)\exp[ik\rho(x_0, y_0; x_1, y_1)]\,dx_0 dy_0\,, \tag{2.1.13}$$

where $\rho(x_0, y_0; x_1, y_1) = L + \frac{1}{2L}(x_1 - x_0)^2 + \frac{1}{2L}(y_1 - y_0)^2$ is the distance between the source point (x_0, y_0) and the observation point (x_1, y_1) in the free space. This result can be extended to the case where the intervening medium consists of a cascade of paraxial and axially symmetric components, which can be described by an overall *ABCD* matrix. And the simplified result can be expressed as

$$\rho(x_0, y_0; x_1, y_1) = \sum_i n_i L_i + \frac{1}{2B}\left(A(x_0^2 + y_0^2) + D(x_1^2 + y_1^2) - 2x_0 x_1 - 2y_0 y_1\right), \tag{2.1.14}$$

Finally, the *Fresnel-Kirchhoff diffraction integral* can be expressed by *ABCD* matrix elements as

$$\begin{aligned} f_1(x_1, y_1) &= -\frac{ik_0}{2\pi B}\exp(ik_0 L) \\ &\cdot \iint f_0(x_0, y_0)\exp\left\{\frac{ik_0}{2B}\left[A\left(x_0^2 + y_0^2\right) - 2x_0 x_1 - 2y_0 y_1 + D\left(x_1^2 + y_1^2\right)\right]\right\} dx_0 dy_0 \end{aligned}\,. \tag{2.1.15}$$

where $k_0 = \frac{2\pi}{\lambda} = \frac{\omega}{c}$ =wave number in vacuum and

$L = \sum_i n_i L_i = optical\ path\ length\ along\ the\ axis$.

Then we transform the Cartesian coordinate *(x, y, z)* to cylindrical coordinate *(*ρ, θ*, z)*. We assumed $x_1 = \rho_1 \cos\theta_1$, $y_1 = \rho_1 \sin\theta_1$, $x_0 = \rho_0 \cos\theta_0$, and $y_0 = \rho_0 \sin\theta_0$, then introduce these parameters into Eq. (2.1.15) and considered $\theta_1 = 0$ [7]

$$\begin{aligned} E(\rho_1, 0) &= -\frac{i}{\lambda B}e^{ikL} \\ &\cdot \int_{\rho_0=0}^{\infty} E_0(\rho_0, \theta_0)\exp\left[\frac{ik}{2B}\left(A\rho_0^2 + D\rho_1^2\right)\right]\rho_0\, d\rho_0 \int_{\theta_0=0}^{\infty} Exp\left[-\frac{ik}{B}\rho_0\rho_1\cos\theta_0\right] d\theta_0 \end{aligned}\,, \tag{2.1.16}$$

From the integral formula on the Bessel function,

$$\int_0^{2\pi} \exp(ix\sin\theta)\,d\theta = \int_0^{2\pi} J_0(x)\,d\theta = 2\pi\, J_0(x)\,, \tag{2.1.17}$$

the cylindrical coordinate *Fresnel Kirchhoff's diffraction integral* can be expressed as

$$E(\rho_1) = -\frac{i2\pi}{\lambda B} e^{ikL} \int_{\rho_0=0}^{\infty} E_0(\rho_0, \theta_0) \exp\frac{ik}{2B}\left(A\rho_0^2 + D\rho_1^2\right) \rho_0 J_0\left(\frac{k\rho_0\rho_1}{B}\right) d\rho_0 . \quad (2.1.18)$$

2.1.2 Input Source Field

In this work, we used supercontunuum light instead of the common single wavelength light source before. Supercontinuum light source is generated by launching an ultrashort pulse from Ti: sapphire pulse laser coupled into a microstructured fiber. Before passing through the axicon element, we collimated the supercontinuum light from the output of microstructured fiber by a microscope objective 40X. And the three dimension and cross-section intensity distribution of collimated light on axicon is shown in Figure 2.7.

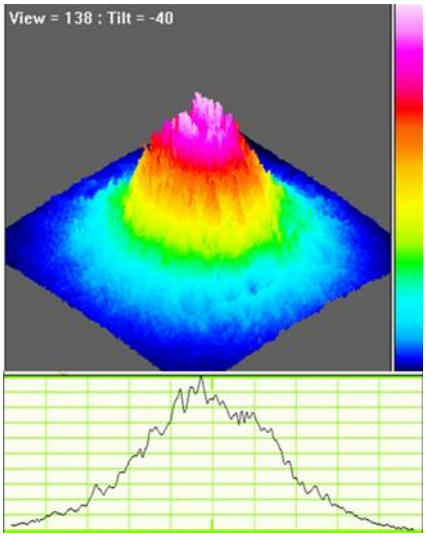

Fig. 2.7 3D and 2D distribution of input beam.

Obviously we can observe the light pattern as a Gaussian distribution, therefore the input light field from axicon element can be expressed as:

$$E(r) = E_0 e^{-\frac{r^2}{w_0^2}}, \quad (2.1.19)$$

Where E_0 is the amplitude of field, w_0 is the spot size, and r is represented as distance from the axis of axicon. In this work, we estimated the spot size w_0 is 2.4 mm from the data.

2.1.3 Theoretical Calculation

The bottle beam with dark center intensity distribution, ring shaped, is generated from the assembly of an axicon with a positive lens. The diameters of the ring shapes are gradually changed as beam propagating along axis. A tendency of ring diameter is increasing at the positions of Z_1, beginning position, to Z_b, and then decreasing from the positions of Z_b to Z_2, end position, shown in Figure 2.8.

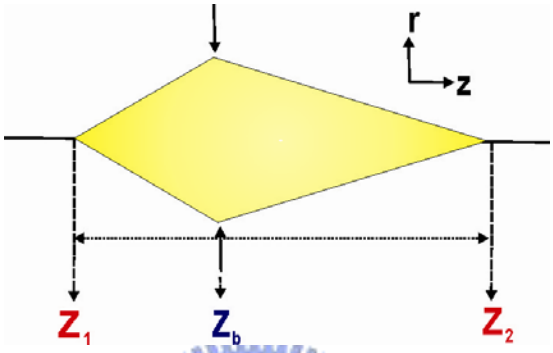

Fig. 2.8 Range of optical bottle beam from Z_1 to Z_2.

In this section, we focused on the bottle beam generated by a Gaussian beam impinging through an axicon and a positive lens. We can roughly estimate the positions of Z_1 and Z_2 by *Fresnel-Kirchhoff's diffraction integral* with the input source field means Gaussian beam field, as shown in Figure 2.9.

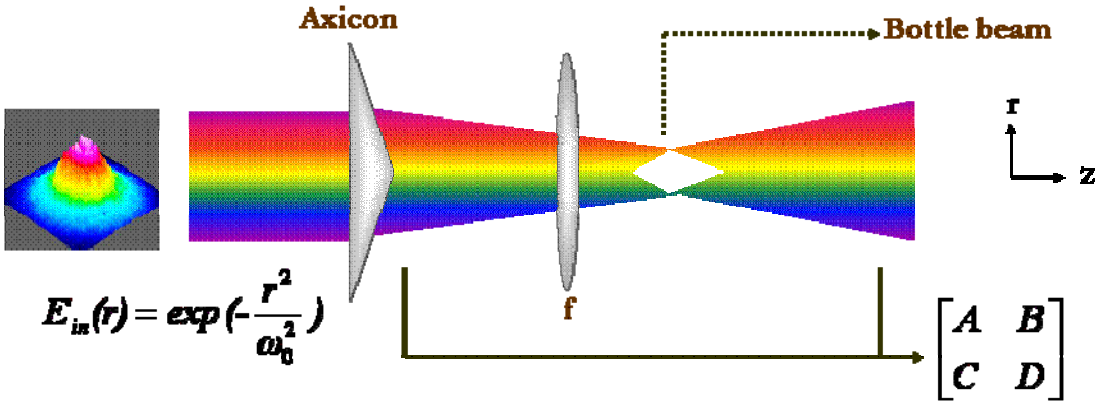

Fig. 2.9 Calculations of optical bottle beam.

We considered the input Gaussian beam $E_{in}(r)$ is given by equation (2.1.19), then passing through an axicon, which created a phase shift a linear profile, that is

$$\tau(r) = Exp(-ik\xi r), \tag{2.1.20}$$

where $\xi = (n-1)\tan\gamma$, n is the refractive index of axicon, and γ is the angle of axicon's cone. When we located a positive lens with a focal length being f beyond the axicon a distance z_0, the diffraction field $E(r', z')$ at a distance z' from the lens can be obtained from *the Fresnel-Kirchhoff's diffraction integral* of cylindrical coordinate, (r', z'), given by

$$E(r', z') = -\frac{i2\pi}{\lambda B} e^{ikL} \int_{r=0}^{\infty} exp\left(-\frac{r^2}{w_0^2}\right) J_0\left(\frac{kr'r}{B}\right) exp\left[\frac{ik}{2B}\left(Ar^2 + Dr'^2\right) - ik\xi r\right] rdr, \tag{2.1.21}$$

Where A, B, D are the elements of the transform ABCD matrix from the axicon through the lens to the distance z'. For the on-axis points $r'=0$ and equation (2.1.21) is simplifies to

$$E(0, z') = -\frac{i2\pi}{\lambda B} e^{ikL} \int_{r=0}^{\infty} exp\left(-\frac{r^2}{w_0^2}\right) exp\left(\frac{ik}{2B} Ar^2 - ik\xi r\right) rdr. \tag{2.1.22}$$

With the integral formula is given by

$$\int_{x=0}^{\infty} x\, exp(-\mu x^2 - 2\nu x)dx = \frac{1}{2\mu} - \frac{\nu}{2\mu}\sqrt{\frac{\pi}{\mu}} exp\left(\frac{\nu^2}{\mu}\right)\left(1 - \Phi\left(\frac{\nu}{\sqrt{\mu}}\right)\right), \tag{2.1.23}$$

Where Φ is the error function. By setting $\mu = \frac{1}{w_0^2} - i\frac{kA}{2B}$, and $\nu = i\frac{k\xi}{2}$, we can obtain the on-axis field to be

$$E(0, z') = -\frac{i2\pi}{\lambda B} e^{ikl}\left\{\frac{1}{2\mu} - \frac{ik\xi}{4\mu}\sqrt{\frac{\pi}{\mu}} exp\left[\frac{(k\xi)^2}{4\mu}\right]\left[1 - \Phi\left(\frac{ik\xi}{2\sqrt{\mu}}\right)\right]\right\}, \tag{2.1.24}$$

Try to introduce the physical parameters into the equation (2.1.24), are given by w_0=2.4 mm, z_0=72 mm, γ=5^0, f=35.08 mm (focal length of the lens), and n=1.51392 at central wavelength λ=670 nm. And the relation between on-axis intensity and distance z' is

plotted in Figure 2.10.

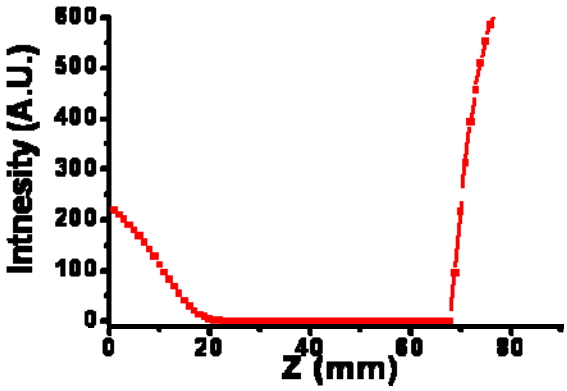

Fig. 2.10 The diagram of on-axis intensity along propagation.

From the Figure 2.10, we can observe two zero-points from relation of on-axis electric intensity and propagated distance, and it means the positions of generating and disappearing, Z_1 and Z_2, respectively. Therefore, we get the data of Z_1 and Z_2 are 25.57 mm and 66.84 mm, respectively.

Besides, fixed previous parameters, we decreased both angle of axicon's cone angle γ and focal length to 0.5^0 and 5.08 mm, the results of Z_1 and Z_2 are about 5.1 mm and 5.4 mm, respectively. This means the range of optical bottle beam can be minimized to micro-meter region when reducing the focal length of the lens or other physical parameter for atom trapping. For different central wavelength light source passing through optical elements, the dispersion effect of axicon and positive lens would be considered, means that refractive index n of axicon element is different with different light source, and the relations of refractive indexes, focal lengths, and light wavelengths we used are shown in Table 2-1.

Table 2.1 Dispersion of refractive index and focal length

Central wavelength (nm)	532	670	780
Refractive index	1.51947	1.51392	1.51116
Focal length of lens (mm)	3.471	3.508	3.527

2.2 Supercontinuum Generation in MFs

Nonlinear effects are the major physical mechanisms leading to the supercontinuum generation in the microstructured fibers. Due to the tailorable dispersion profile of microstructured fiber, the high nonlinear coefficient and the suitable zero-dispersion point can be made. The diagram of microstructured fiber is shown in Figure 2.11.

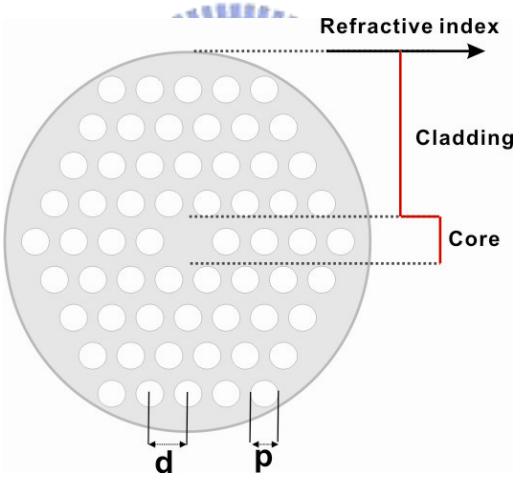

Fig. 2.11 Structure of the microstructure fiber.

When the high peak power pulses propagate in the fiber, several nonlinear effects can be easily induced. These nonlinear phenomena include self-phase modulation (SPM), degenerate four-wave mixing (DFWM), stimulated Raman scattering (SRS), self-steepening (SS), higher-order dispersion (HOD), etc. These major nonlinear effects above will be briefly described in the followings.

Self-phase modulation (SPM) is a physical phenomenon that broadened spectrum of

propagating pulses in fiber. With enough input power, the refractive index of a nonlinear medium is dependent on the optical intensity. The refractive index can be expressed as

$$n = n_L + n_2 |A|^2, \tag{2.2.1}$$

where n_L is the linear part of the refractive index, n_2 is the nonlinear index of refractive, and $|A|^2$ is the optical intensity. With a pulse propagating, the SPM effect induce the nonlinear phase shift in the fiber as

$$\phi_{NL}^{SPM}(T) = \frac{2\pi L}{\lambda} n_2 |A(T)|^2, \tag{2.2.2}$$

where L is the length of the fiber, λ is the wavelength. This nonlinear phase shift can induce a frequency chirp that leads the spectral broadening of the pulse.

Degenerate four-wave mixing (DFWM) is a process that two pump photons generate a Stokes photon (lower frequency) and an anti-Stokes photon (higher frequency) when the phase-matching condition is satisfied, expressed as

$$2\omega_p \rightarrow \omega_s + \omega_{as}, \tag{2.2.3}$$

where ω_p, ω_s, and ω_{as} are the pumping photon, Stokes photon, and anti-Stokes photon, respectively.

Stimulated Raman scattering (SRS) is an interaction between photon and phonon. It is described quantum-mechanically as scattering of a photon by one of the molecules to a lower-frequency photon, while the molecule makes transition to a higher energy vibration state. This effect will induce the pulse spectrum shifts toward the low-frequency side as the pulse propagates inside the fiber.

Self-steepening (SS) is originated from the intensity of the group velocity dispersion, the peak of the pulse moves at a slower velocity than the wings which induces the trailing edge of the pulse to become steeper as the pulse propagation. The SS effect leads to an asymmetry in the SPM-broadened spectra of ultra-short pulses.

Higher-order dispersion (HOD) effect becomes important in optical fibers when the

carrier frequency is close to the zero-dispersion point.

2.3 Vectorial Field Theory

From the scalar diffraction theory, *Fresnel-Kirchhoff's diffraction integrals*, the traverse field would be obtained with neglecting the longitudinal field. Although optical particle trapping is needed to be in the micro-sized region, the high numerical-aperture microscope objective to focus the optical beam would be needed in optical trapping system. The total trapping force acting on a transparent spherical particle related to the polarization of the incident light is reported [36] [37]. In this section, the *Vectorial Rayleigh diffraction integrals* will be discussed to calculate the vectorial electric field of specific input polarization light including traverse and longitudinal fields.

2.3.1 Vectorial Rayleigh Diffraction Integrals

In a homogeneous medium, the forward monochromatic propagating vector field $\boldsymbol{E}(r_\perp, z)$ can be related to its distribution on the plane $z = 0$ (exit pupil plane) by means of relations [38] [39].

$$\tilde{E}_\perp(\tilde{r}_\perp, z) = -\frac{1}{2\pi}\int d^2 r_0 \tilde{E}(\tilde{r}_0, 0)\frac{\partial}{\partial z}\left(\frac{exp(ikR)}{R}\right), \tag{2.3.1}$$

$$E_z(\tilde{r}_\perp, z) = \frac{1}{2\pi}\int d^2 r_0 \left[E_x(\tilde{r}_0, 0)\frac{\partial}{\partial x}\left(\frac{exp(ikR)}{R}\right) + E_y(\tilde{r}_0, 0)\frac{\partial}{\partial y}\left(\frac{exp(ikR)}{R}\right)\right], \tag{2.3.2}$$

where $\tilde{r}_\perp = x\hat{i} + y\hat{j}$, $\tilde{r}_0 = x_0\hat{i} + y_0\hat{j}$, $\tilde{E}_\perp = E_x\hat{i} + E_y\hat{j}$, k is the wave number, and

$$R = \sqrt{(x - x_0)^2 + (y - y_0)^2 + z^2}\ .$$

These vectorial diffraction equations can be derived in the developed "*m-theory*" solutions that satisfy *Maxwell's* equations [40], whose boundary values are reproduced when the observation point, where the field is calculated, is chosen on the plane. Recall that the expression for the *m-theory* integral as

$$\widetilde{E}(Q) = 2\int_{\Sigma}\left[\widetilde{m}\times\widetilde{E}(P)\right]\times\nabla G(P,Q)\,d\Sigma\,, \tag{2.3.3}$$

where Q means observation point, P means source point, G is the *Green* function, defined as $\dfrac{exp\left(ik\left|\widetilde{Q}-\widetilde{P}\right|\right)}{4\pi\left|\widetilde{Q}-\widetilde{P}\right|}$, and $\boldsymbol{m}$ is the normal vector on the interface Σ points in the positive z direction.

Török et al. [41] expressed the electric and magnetic vectors in the exit pupil plane by means of a matrix formalism. For the usual assumption are made, that the electric vector maintains its direction with respect to a meridional plane and the electric vector remains on the same side of a meridional plane on passing through the system; the demonstrated model is shown in Figure 2.12.

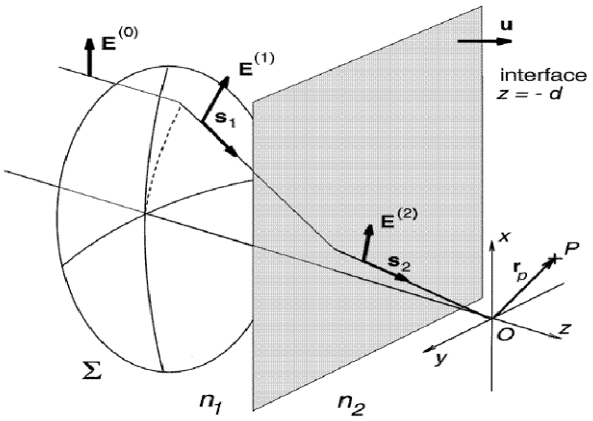

Fig. 2.12 Demonstrated model of *Török* et al.

The used model is that a polarized light $\boldsymbol{E}^{(0)}$ passed through a lens and a material whose refractive index is different from that of the medium of the propagation in placed into the image space. Assuming the incident electric vector $\boldsymbol{E}^{(0)}$ in front of the lens is expressed as

$$\widetilde{E}^{(0)} = \left[E_x^0 \quad E_y^0 \quad 0\right]^T, \tag{2.3.4}$$

T means transport matrix. After passing the lens, the treatment of the refraction is to decompose the electric vector into *s*- and *p*-polarized vector components E_s and E_p,

respectively, and to rotate the coordinate system to the new coordinate system (p,s,ζ). Therefore, the electric vector after the lens can be expressed as

$$E^{(1)}_{(p,s,\varsigma)} = A(\theta_1)P^{(1)}LRE^{(0)}_{(x,y,z)}, \tag{2.3.5}$$

where $A(\theta_1)$ is an amplitude function (defined below), and $\mathbf{P^{(1)}}$, **L**, **R** mean rotation matrices. The matrix **R** describes the coordinate transformation for rotation around z axis; the matrix **L** describes the changes in the electric field as it traverses the lens; and $\mathbf{P^{(1)}}$ describes the coordinate system rotation that generate E_s and E_p components with E_ζ =0. They are expressed as

$$R = \begin{bmatrix} \cos\phi & \sin\phi & 0 \\ -\sin\phi & \cos\phi & 0 \\ 0 & 0 & 1 \end{bmatrix}, \; L = \begin{bmatrix} \cos\theta_1 & 0 & \sin\theta_1 \\ 0 & 1 & 0 \\ -\sin\theta_1 & 0 & \cos\theta_1 \end{bmatrix}, \; P^{(1)} = \begin{bmatrix} \cos\theta_1 & 0 & -\sin\theta_1 \\ 0 & 1 & 0 \\ \sin\theta_1 & 0 & \cos\theta_1 \end{bmatrix}, \tag{2.3.6}$$

where θ_1 is focus angle of lens, and ϕ is the azimuth angle of spherical coordinate.

The electric field in the second material, $E^{(2)}$ is given by

$$E^{(2)}_{(x,y,z)} = R^{-1}\left[P^{(2)}\right]^{-1} IE^{(1)}_{(p,s,\zeta)}. \tag{2.3.7}$$

Here the matrix **I** describes the effect of the interface between two media, the matrix $[\mathbf{P}^{(2)}]^{-1}$ describes the rotation of the coordinate system required to return it to the (p,s,z) system, and matrix $\mathbf{R}^{-1}$ describes the inverse rotation around the z axis.

$$I = \begin{bmatrix} \tau_p & 0 & 0 \\ 0 & \tau_s & 0 \\ 0 & 0 & \tau_p \end{bmatrix}, \; \left[P^{(2)}\right]^{-1} = \begin{bmatrix} \cos\theta_2 & 0 & \sin\theta_2 \\ 0 & 1 & 0 \\ -\sin\theta_2 & 0 & \cos\theta_2 \end{bmatrix}, \tag{2.3.8}$$

in which τ_p and τ_s are the Fresnel coefficients,

$$\tau_s = \frac{2\sin\theta_2\cos\theta_1}{\sin(\theta_1+\theta_2)}, \text{ and } \tau_p = \frac{2\sin\theta_2\cos\theta_1}{\sin(\theta_1+\theta_2)\cos(\theta_1-\theta_2)}, \tag{2.3.9}$$

where θ_2 is the refraction angle of the second medium. The function $A(\theta_1)$ can be regarded as an function that depends on the lens used in imaging. Richards and Wolf [42] showed that when the system obeys Abbe's sine condition, i.e., is aplanatic, then

$$A(\theta_1) = fA_0 \cos^{1/2}\theta_1 , \tag{2.3.10}$$

where f is the focal length of the lens and A_0 is input amplitude factor. And the influence of phase factor through optical system would be considered into the amplitude function to describe the field. By the combination of the electric matrix forms from *Török* as input electric field and *Vectorial Rayleigh diffraction integral*, the traverse and longitudinal electric field would be obtained.

2.3.2 Vectorial Field Calculation

In this work, there is an assembly of an axicon with a lens of the optical system to be discussed. At first, the *Vectorial Rayleigh diffraction integrals* can be simplified by expanding R of Eqs. (2.3.1~2) into a series and keeping only the first and the second terms, i.e.,

$$R \approx r + \frac{x_0^2 + y_0^2 - 2xx_0 - 2yy_0}{2r}, \tag{2.3.11}$$

where $r = (x^2+y^2+z^2)^{1/2}$, and we can obtain the following vectorial integrals in the cylindrical coordinate:

$$E_x(\rho,\beta,z) = -\frac{iz\exp(ikr)}{\lambda r^2}\int_0^{\infty} d\rho_0 \int_0^{2\pi} d\phi\, E_x(\tilde{r}_0)\exp\left(ik\frac{\rho_0^2}{2r}\right)\exp\left(-ik\frac{\rho\rho_0\cos(\phi-\beta)}{r}\right)\rho_0 ,$$

(2.3.12)

$$E_y(\rho,\beta,z) = -\frac{iz\exp(ikr)}{\lambda r^2}\int_0^{\infty} d\rho_0 \int_0^{2\pi} d\phi\, E_y(\tilde{r}_0)\exp\left(ik\frac{\rho_0^2}{2r}\right)\exp\left(-ik\frac{\rho\rho_0\cos(\phi-\beta)}{r}\right)\rho_0 ,$$

(2.3.13)

$$E_z(\rho,\beta,z) = -\frac{i\exp(ikr)}{\lambda r^2}\int_0^{\infty} d\rho_0 \int_0^{2\pi} d\phi \left[E_x(\tilde{r}_0)(\rho\cos\beta - \rho_0\cos\phi) + E_y(\tilde{r}_0)(\rho\sin\beta - \rho_0\sin\phi)\right] \times \exp\left(ik\frac{\rho_0^2}{2r}\right)\exp\left(-ik\frac{\rho\rho_0\cos(\phi-\beta)}{r}\right)\rho_0 ,$$

(2.3.14)

where (ρ,β,z) are the cylindrical coordinates of the polar points at the point of observation, (ρ_0, ϕ) are the polar coordinates on the plane of the exit pupil, and $\boldsymbol{E}(r_0)$ is the field immediately behind the assembly of an axicon and a lens. Recently, the electric vector form of axicon and its vectorial diffraction field distribution have been demonstrated [43]. We will derive the vectorial field in combination of axicon and lens as the followings.

Assuming the field immediately behind the assembly $\boldsymbol{E}(r_0)$ can be written as

$$\widetilde{E}(\widetilde{r}_0) = \begin{bmatrix} E_x(\widetilde{r}_0) \\ E_y(\widetilde{r}_0) \\ E_z(\widetilde{r}_0) \end{bmatrix} = \widetilde{P}(\phi)A(\rho_0,\phi), \tag{2.3.15}$$

where $P(\phi)$ is the polarization and $A(\rho_0, \phi)$ represents the complex amplitude at the exit pupil. Then we assumed an incident polarized light, which in general, depend on the polar angle ϕ:

$$P_0 = \begin{bmatrix} a(\phi) \\ b(\phi) \\ 0 \end{bmatrix}. \tag{2.3.16}$$

From the method presented by *Török* et al. to describe the axicon polarization vector as:

$$P(\phi) = M_{Lens} \cdot M_{Axicon} \cdot P_0 = \left(R^{-1}P(\theta_1)^{-1}IP(\theta_1)L(\theta_1)R\right)\cdot\left(R^{-1}L^{-1}I_{axicon}LCR\right)\cdot P_0 \ ,$$

where the matrix M_{Lens} is obtained by assuming θ_1 is equal to θ_2 and **I** is the unit matrix in Eqs. (2.3.7) and (2.3.8), respectively. Besides, $\mathbf{M}_{Axicon}$ is demonstrated by [43] in Figure 2.13, in which the matrix **R** describes the rotation of the coordinate system around the optical axis, **C** describes the change of polarization through the axicon, **L** describes a rotation of the coordinate system into *s*- and *p*- polarized vectors, and $\mathbf{I}_{Axicon}$ represents the transmission (Fresnel coefficients) through slope of the axicon, shown in the followings:

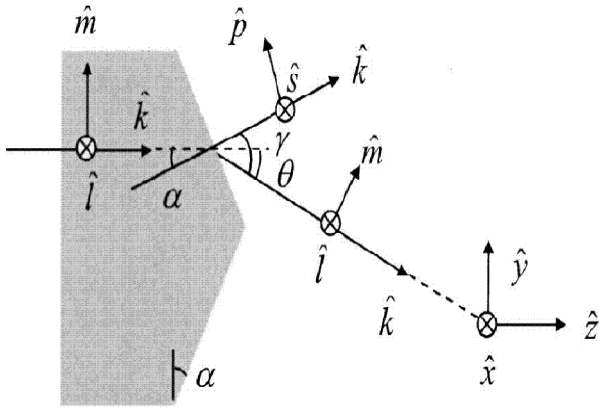

Fig. 2.13 Schematic overview of the natural basis (k,l,m), polarization basis (k,s,p), and Cartesian basis (x,y,z).

$$C=\begin{bmatrix} \cos\theta & 0 & \sin\theta \\ 0 & 1 & 0 \\ -\sin\theta & 0 & \cos\theta \end{bmatrix},\quad L=\begin{bmatrix} \cos\alpha & 0 & -\sin\alpha \\ 0 & 1 & 0 \\ \sin\alpha & 0 & \cos\alpha \end{bmatrix},\quad I_{Axicon}=\begin{bmatrix} t_p & 0 & 0 \\ 0 & t_s & 0 \\ 0 & 0 & t_p \end{bmatrix}$$

$$M_{Axicon}=\begin{bmatrix} a(t_p\cos\theta\cos^2\phi+t_s\sin^2\phi)+b(t_p\cos\theta-t_s)\sin\phi\cos\phi \\ a(t_p\cos\theta-t_s)\sin\phi\cos\phi+b(t_p\cos\theta\sin^2\phi+t_s\cos^2\phi) \\ -at_p\sin\theta\cos\phi-bt_p\sin\theta\sin\phi \end{bmatrix}, \tag{2.3.17}$$

where angle θ is shown in Figure 2.13, τ_p and τ_s are the Fresnel coefficients.

The polarization vector P(ϕ) behind the lens is the M_{Axicon} that θ is replaced by $\theta+\theta_1$, where θ_1 is the focus angle of the lens depends on parameters ρ_0 and θ from *ABCD* matrix theory, shown in Figure 2.14.

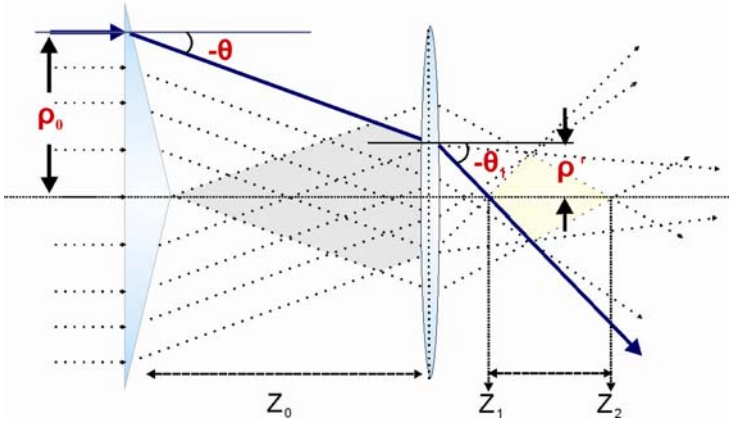

Fig. 2.14 Assembly of axicon and a lens.

Here *ABCD* matrix can be shown as:

$$\begin{bmatrix} \rho' \\ -\theta_1 \end{bmatrix} = \begin{bmatrix} 1 & 0 \\ -\frac{1}{f} & 1 \end{bmatrix} \begin{bmatrix} 1 & Z_0 \\ 0 & 1 \end{bmatrix} \begin{bmatrix} \rho_0 \\ -\theta \end{bmatrix} = \begin{bmatrix} \rho_0 - Z_0\,\theta \\ -\frac{\rho_0}{f} - \theta(1-\frac{Z_0}{f}) \end{bmatrix}. \tag{2.3.18}$$

Then we assume $A(\rho_0,\varphi)$ included amplitude and phase distribution terms at the exit pupil as:

$$\mathrm{A}(\rho_0,\phi) = \exp\left(-\frac{\rho_0^{\,2}}{w^2}\right)\exp\left(-\mathrm{ik}\xi\rho_0\right)\ \exp(-\mathrm{ik}\frac{\rho'^2}{2\mathrm{f}})\ \mathrm{rect}\left(\frac{\rho_0}{\mathrm{R}}\right)\ \cos^{1/2}\theta_1(\rho_0)\ , \tag{2.3.19}$$

where w is the spot size, $\xi = (n-1)\tan\gamma$, γ is conical angle of axicon, f is focal length of lens, and R is the radius of the circular aperture. Then we introduce amplitude and phase terms in the exit pupil ($z = 0$) into the *Vectorial Rayleigh diffraction Integrals* (Eqs. 2.3.12~17) and consider the specific incident polarized field, radial polarized and linear polarized (x-polarized) field, respectively.

(1) *Radial-polarized field* ($a = \cos\phi$, $b = \sin\phi$)

The field distribution of the *radial-polarized field* behind the lens ($z = 0$) can be expressed as

$$E_x(\rho,\beta,z) = -\frac{kzt_p\exp(ikr)}{r^2}\cos\beta\int_0^R d\rho_0\rho_0\ \exp\left(-\frac{\rho_0^2}{\omega^2}\right)\exp\left[ik\left(\frac{\rho_0^2}{2r} - \xi\rho_0 - \frac{(\rho_0 - Z_0\theta)}{2f}\right)\right]$$
$$\times J_1\left(\frac{k\,\rho\rho_0}{r}\right)\cos\left[(2-\frac{Z_0}{f})\theta + \frac{\rho_0}{f}\right]\cos^{1/2}\left[(1-\frac{Z_0}{f})\theta + \frac{\rho_0}{f}\right] \tag{2.3.20}$$

$$E_y(\rho,\beta,z) = -\frac{kzt_p\exp(ikr)}{r^2}\sin\beta\int_0^R d\rho_0\rho_0\ \exp\left(-\frac{\rho_0^2}{\omega^2}\right)\exp\left[ik\left(\frac{\rho_0^2}{2r} - \xi\rho_0 - \frac{(\rho_0 - Z_0\theta)}{2f}\right)\right]$$
$$\times J_1\left(\frac{k\,\rho\rho_0}{r}\right)\cos\left[(2-\frac{Z_0}{f})\theta + \frac{\rho_0}{f}\right]\cos^{1/2}\left[(1-\frac{Z_0}{f})\theta + \frac{\rho_0}{f}\right] \tag{2.3.21}$$

$$E_z(\rho,\beta,z)=\frac{ikt_p exp(ikr)}{r^2}\int_0^R d\rho_0\rho_0\ exp\left(-\frac{\rho_0^2}{\omega^2}\right)exp\left[ik\left(\frac{\rho_0^2}{2r}-\xi\rho_0-\frac{(\rho_0-Z_0\theta)}{2f}\right)\right]$$
$$\times\left[\rho_0 J_0\left(\frac{k\rho\rho_0}{r}\right)+i\rho_1 J_0\left(\frac{k\rho\rho_0}{r}\right)\right]cos\left[(2-\frac{Z_0}{f})\theta+\frac{\rho_0}{f}\right]$$
$$\times cos^{1/2}\left[(1-\frac{Z_0}{f})\theta+\frac{\rho_0}{f}\right] \qquad (2.3.22)$$

(2) *Linear x-polarized field (a=1,b=0)*

The field distribution of the *linear x-polarized field* behind the lens ($z = 0$) can be expressed as:

$$E_x(\rho,\beta,z)=-\frac{ikzexp(ikr)}{2r^2}\int_0^R d\rho_0\rho_0\ exp\left(-\frac{\rho_0^2}{\omega^2}\right)exp\left[ik\left(\frac{\rho_0^2}{2r}-\xi\rho_0-\frac{(\rho_0-Z_0\theta)}{2f}\right)\right]$$
$$\times\left[\left(t_p cos\left[(2-\frac{Z_0}{f})\theta+\frac{\rho_0}{f}\right]+t_s\right)J_0\left(\frac{k\rho\rho_0}{r}\right)-\left(t_p cos\left[(2-\frac{Z_0}{f})\theta+\frac{\rho_0}{f}\right]-t_s\right)\right.$$
$$\left.\times J_2\left(\frac{k\rho\rho_0}{r}\right)cos2\beta\right]cos^{1/2}\left[(1-\frac{Z_0}{f})\theta+\frac{\rho_0}{f}\right] \qquad (2.3.23)$$

$$E_y(\rho,\beta,z)=-\frac{ikzexp(ikr)}{2r^2}sin2\beta\int_0^R d\rho_0\rho_0\ exp\left(-\frac{\rho_0^2}{\omega^2}\right)exp\left[ik\left(\frac{\rho_0^2}{2r}-\xi\rho_0-\frac{(\rho_0-Z_0\theta)}{2f}\right)\right]$$
$$\times\left(t_p cos\left[(2-\frac{Z_0}{f})\theta+\frac{\rho_0}{f}\right]-t_s\right)J_2\left(\frac{k\rho\rho_0}{r}\right)cos^{1/2}\left[(1-\frac{Z_0}{f})\theta+\frac{\rho_0}{f}\right] \qquad (2.3.24)$$

$$E_z(\rho,\beta,z)=-\frac{ikexp(ikr)}{2r^2}cos\beta\int_0^R d\rho_0\rho_0\ exp\left(-\frac{\rho_0^2}{\omega^2}\right)exp\left[ik\left(\frac{\rho_0^2}{2r}-\xi\rho_0-\frac{(\rho_0-Z_0\theta)}{2f}\right)\right]$$
$$\left[\left(t_p cos\left[(2-\frac{Z_0}{f})\theta+\frac{\rho_0}{f}\right]+t_s\right)\rho J_0\left(\frac{k\rho\rho_0}{r}\right)-\left(t_p cos\left[(2-\frac{Z_0}{f})\theta+\frac{\rho_0}{f}\right]\right.\right.$$
$$\left.\left.-t_s\right)\rho J_2\left(\frac{k\rho\rho_0}{r}\right)+2it_p\rho_0 cos\left[(2-\frac{Z_0}{f})\theta+\frac{\rho_0}{f}\right]J_1\left(\frac{k\rho\rho_0}{r}\right)\right]$$
$$\times cos^{1/2}\left[(1-\frac{Z_0}{f})\theta+\frac{\rho_0}{f}\right] \qquad (2.3.25)$$

Here $J_m(x)$ is the m-th Bessel function of the fist kind. And the above equations are obtained by using integral functions to Eqs. (2.3.12~14) as:

$$\int_0^{2\pi} d\phi \, cosm\phi \, exp[i\eta cos(\phi - \beta)] = 2\pi i^m J_m(\eta) cosm\beta \,, \tag{2.3.26}$$

$$\int_0^{2\pi} d\phi \, sinm\phi \, exp[i\eta cos(\phi - \beta)] = 2\pi i^m J_m(\eta) sinm\beta \,. \tag{2.3.27}$$

Since the above vectorial field equations could not be analytically calculated, it needs to numerically solve them. We used the Simpson's approximation, an integral approximation that uses quadratic polynomials to fit the integral solution, shown in the following:

$$\int_a^b f(x)dx \approx \frac{b-a}{3n}\left(f(x_0) + 4\sum_{k=1,3,5...}^{n-1} f(x_k) + 2\sum_{m=2,4,6...}^{n-2} f(x_m) + f(x_n) \right), \tag{2.3.28}$$